Molecular Crystals and Liquid Crystals

Publication details, including instructions for authors and subscription information:
http://www.tandfonline.com/loi/gmcl20

Influence of Hydrogen Bonding on Device Parameters and Field Response in N* and SmC* Phases of a Ferroelectric Liquid Crystal, HBFLC: 12 bpa

B. Sreedevi [a], P. V. Chalapathi [a], V. K. M. Kotikalapudi [a], V. G. K. M. Pisipati [b] & D. M. Potukuchi [a]

[a] Department of Physics, Jawaharlal Nehru Technological University, Kakinadaand University College of Engineering, Kakinada, India

[b] Koneru Lakshmaiah College of Engineering, Vaddeswaram, India

Version of record first published: 17 Dec 2009

To cite this article: B. Sreedevi, P. V. Chalapathi, V. K. M. Kotikalapudi, V. G. K. M. Pisipati & D. M. Potukuchi (2009): Influence of Hydrogen Bonding on Device Parameters and Field Response in N* and SmC* Phases of a Ferroelectric Liquid Crystal, HBFLC: 12 bpa, Molecular Crystals and Liquid Crystals, 515:1, 71-98

To link to this article: http://dx.doi.org/10.1080/15421400903290378

Mol. Cryst. Liq. Cryst., Vol. 515, pp. 71–98, 2009

ISSN: 1542-1406 print/1563-5287 online
DOI: 10.1080/15421400903290378

Influence of Hydrogen Bonding on Device Parameters and Field Response in N* and SmC* Phases of a Ferroelectric Liquid Crystal, HBFLC: 12 bpa

B. Sreedevi[1], P. V. Chalapathi[1], V. K. M. Kotikalapudi[1], V. G. K. M. Pisipati[2], and D. M. Potukuchi[1]
[1]Department of Physics, Jawaharlal Nehru Technological University, Kakinada, and University College of Engineering, Kakinada, India
[2]Koneru Lakshmaiah College of Engineering, Vaddeswaram, India

Isotropic to chiral nematic (IN) and chiral nematic to chiral SmC(N*C*) transitions are studied by LF dielectric method in a hydrogen bonded ferroelectric liquid crystal, viz., 12 bpa. They agree with TM and DSC reports. Tilt angle, electro-clinic effect, spontaneous polarization, and dielectric relaxations are investigated and compared with that of an odd homologue 11 bpa. Growth of tilt and spontaneous polarization as order parameters in SmC* phase agree with mean-field prediction. Effect of H-bonding on the growth of tilt and P_S order parameters is discussed. Observed large EC-effect is explained by the inclined configuration of soft-covalent interaction. Dielectric dispersion revealed a collective response, viz., Goldstone mode at ~100 Hz in SmC* and an LF-mode in N* phases. The two HF-relaxations, i.e., Types I and II in N* and SmC* phases are explained through a refined dipole model. Shift of GM with field in SmC* is explained. Off-centred dispersion is explained through the Cole-Davidson relation. HF relaxations are related to the individual dipole reorientation. Shift of f_R with T infers higher activation energy for Type I and lower activation energy for Type II relaxations. Soft mode permittivity follows the Curie–Weiss law in the vicinity of $T_{N^*C^*}$. Device parameters, viz., thermal stability, tilt angle, and spontaneous polarization in SmC* phase are found to be influenced by H-bonding in FLCs. Results are is discussed and compared with the data reported on 11 bpa and other FE materials.*

Keywords: activation energy; electroclinic effect; ferroelectric tilt angle; Goldstone mode; hydrogen bonding; relaxation; spontaneous polarization

Address correspondence to D. M. Potukuchi, Department of Physics, University College of Engineering, Jawaharlal Nehru Technological University, Kakinada, 533003, A. P. India. E-mail: potukuchidm@yahoo.com

INTRODUCTION

In liquid crystals (LCs), ferroelectricity is first realized [1] in the chiral tilted smectic version in its surface stabilized (SSFLC) geometry, i.e., in the homogeneously aligned SmC* phase. LCs are important among optical display materials due to their rich Electro-Optic (EO) response. In general, long range orientational order characterizes an LC phase, while smectic phases possess additional layering order. Displays based on nematic phase possessing alone orientational order operate at ms speed, while smectic based devices operate at μ sec speed. From fundamental point of view, tilt angle θ is the primary order parameter, while the spontaneous polarization (P_S) represents the secondary order parameter in FE SmC* phase. The SmC* phase with large tilt angle ensures wide viewing angle for the device. The advantages of SSFLC (in C* phase) devices over the classical nematic devices include [2] faster switching, enhanced bistability and large contrast ratios. The C* based devices are known to have two stable states. It remained an experimental difficulty to obtain the ideal surface stabilised alignment. Recently, it is realised [3–6] that Anti Ferroelectric liquid crystals (AFLCs) exhibit a large tilt angle [7] of 45°. They can be used in tri-stable switching devices in their gray scale mode. Further, it is also noticed that the inherent anti parallel alignment in an AFLC could not adversely affect [8,9] the contrast ratio of the device. In summary, larger is the tilt angle, more is the possibility for the optic axis to align normal to the substrate of the device in the un-switched state. In turn, the un-switched device gives perfect extinction between the crossed polarizers. As a result, an extremely high contrast [10] ratio can be realised. Thus, either an inherently large tilt angle or its tunability (with field) leads to the optimal utilization of SmC* phase in a device. The coupling between an electric field and the molecular tilt is known as Electro-Clinic (EC) effect. The EC-effect is analysed through symmetry arguments [11–13] and is explained in terms of coefficients of Free energy [14–17] expansion. The concept of EC-effect is further developed for its applicability in electro-optic (EO) devices. The continuous variation of tilt with field leads to a gray scale [18–21] mode. Hence, the behaviour of the tilt as a primary order parameter with the field provides valuable data. Further, the identification of N* and SmC* phases gained [22–24] importance, as both of them exhibited V-shaped switching. The V-shaped switching implies a threshold-less operation in gray scale mode. Investigations of LF dielectric relaxations in LC phases in the domain of frequency and dielectric strength provide [25,26] invaluable information regarding the response of dipole moment to the external field. Thus, its response would be preferentially optimized in the devices.

The realization of a chiral smectic or nematic LC phase with high [27] spontaneous polarization P_S, low viscosity η, fast switching time τ_s, tunable tilt angle θ(E) remained a continuous ongoing research effort. Furthermore, the presence of hydrogen bonding (i.e., through its soft-covalent interaction) is known [28] to influence the thermal stability of the phase and spontaneous polarization in the classical inorganic ferroelectric materials.

Hence, it would be useful to carry out a detailed study of tilt, spontaneous polarization, and low-frequency dielectric relaxations in a Hydrogen Bonded Ferroelectric Liquid Crystal (HBFLC) exhibiting N^* and SmC^* phases. Further, the influence of chemical moieties [27] involved in the supra-molecular design [29–34] of the 12 bpa is discussed based on the data reported [35] for 11 bpa. The influence of chiral center and its environment in SmC^* phase are studied in detail to optimize [1] their utility in devices like switches, modulators, and TV screens, etc.

In the present article, the influence of the molecular structure and the presence of H-bonding on the thermal stability of LC phases, the tilt angle and its response to field (viz., FE effect) are investigated. The investigations of the low frequency dielectric relaxations in its chiral N^* and SmC^* phases are presented. A comparative study of the experimental results on 12 bpa and 11 bpa [35] is presented along with the results on other FLCs.

EXPERIMENTAL

The compound 12 bpa was synthesised as reported [36] earlier. The molecular formula for the present HBFLC complex, viz., 12 bpa is given by

$$C_{12}H_{25}O \cdot COOH : HOOC \cdot C^*HBr \cdot CH_3.$$

It is noticed [36] that 12 bpa exhibits the following sequence of phases (in the cooling run) during TM and DSC techniques:

$$\text{Iso} \xrightarrow{128.6^\circ C} N^* \xrightarrow{120.4^\circ C} SmC^* \xrightarrow{78.3^\circ C} SmG^* \xrightarrow{60.8^\circ C} \text{Cr}.$$

The procedure used to fill the sample, control the temperature, estimate the spontaneous polarization [37], and study the LF dielectric response (HP 4192A LF Impedance Analyzer) were similar to those reported [35] earlier. The tilt angle and EC-effect in the SmC^* phase were determined by the optical extinction [38] method. The dielectric cell is calibrated and the lead capacitance ($\sim$2.5 pF) and empty cell capacitance (20 pF) are determined as reported [35] earlier. The lead capacitance and empty cell capacitance were found to be invariant with the temperature (in the range of 30°C–150°C) and frequency

(in the range of 20 Hz–8 MHz). Relatively permittivity (or dielectric constant) ε_r (frequently referred as ε') and dielectric loss ε'' were estimated from capacitance (panel-I) and loss factor Tan δ (from panel-II) as reported [35] earlier.

RESULTS AND DISCUSSION

Determination of Phase Transition Temperatures

The temperature variation of capacitance 'C' and dielectric loss ε'' exhibited by 12 bpa filled cell are presented in Fig. 1. Capacitance is found to accompany with an overall increase, while the loss is found to exhibit a decrease with temperature. The temperature at which capacitance exhibits a peak is identified (inset arrows in Fig. 1) as phase transition temperature. The transition temperatures determined by the dielectric method i.e., 128.6°C for T_{IN^*} and 120.55°C for $T_{N^*C^*}$ are found to agree with the reported [36] values by TM and DSC. Increase in capacitance with decreasing temperature is argued due to the growing dipolar ordering. The over all capacitance in the present 12 bpa is found be less in magnitude (by around 20 pF) than that in 11 bpa. 11 bpa being an odd homologue, projects [39] more transverse dipole moment. Thereby, the surface area swept by molecule increases and the charge bearing capacity increases. The SmC^* to SmG^* transition temperature is not detectable by the present dielectric method as the sample develops breaks at lower temperature due to the increased viscosity.

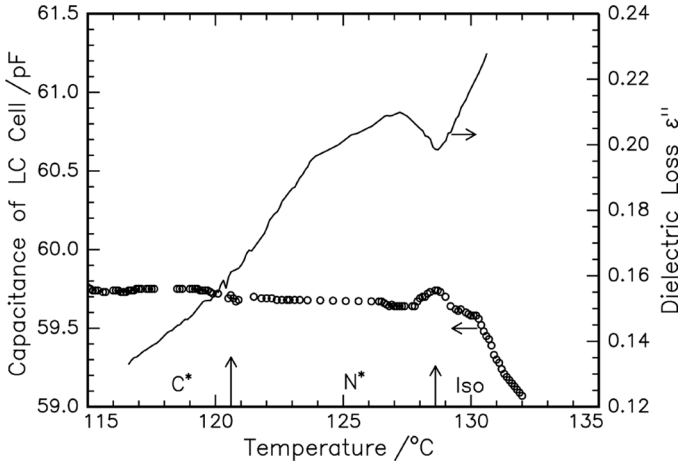

FIGURE 1 Temperature variation of capacitance C(T) exhibtied by 12 bpa filled cell and dielectric loss ε''(T).

Measurement of Tilt Angle in SmC* Phase

The tilt angle is estimated [35,38] as half of the angular displacement of the cell (fixed on the microscope stage) to observe two successive optical extinction positions (for the C* textural domains). The observed temperature variation of tilt angle θ(T) in the SmC* phase is presented in Fig. 2. The tilt angle increases with decreasing temperature in the SmC* phase and attains a maximum value of $\sim$20.2°. Although, the tilt angle in SmC* phase of 12 bpa is not so large a value as reported [7,40,41] recently in other FLC compounds, it falls on the higher side [42,43] of the values. However, the present case of higher value of tilt angle is suggestive [1] of a possible larger viewing angle for SmC* device. The occurrence of large tilt angle in the HBFLC is argued due to the inclined configuration of H-bonding (i.e., soft covalent bond as in Template-1) with respect to the long molecular axis. The observed increase in the tilt angle and the thermal span of SmC* phase in HBFLC agrees with the predictions of Luckhurst's molecular [29] model and Marcelja's theory [39] of axial polarizabilities.

It is also noticed that tilt angle θ(T) in the SmC* phase represents [44,45] the primary order parameter. The growth of tilt order parameter is estimated by fitting the observed data of θ(T) to the relation

$$\theta(\mathrm{T}) \propto (\Delta \mathrm{T})^{\beta_1} \tag{1}$$

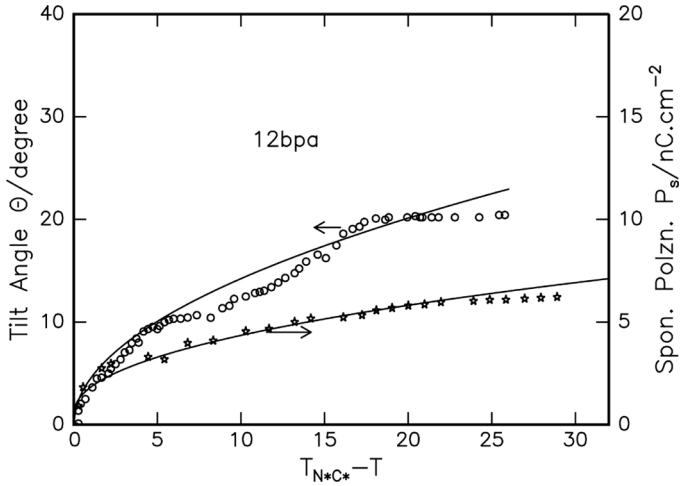

FIGURE 2 Temperature variation of Tilt angle θ(T) and spontaneous polarization P_S(T) exhibited by 12 bpa in SmC* phase.

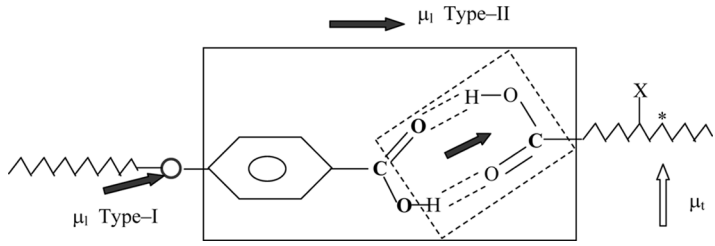

TEMPLATE 1 Refined molecular dipole model for 12 bpa.

where $\Delta T = |T_{N^*C^*} - T_i|$, $T_{N^*C^*}$ is the chiral Nematic to Smectic-C* transition temperature, and T_i is the temperature of interest in SmC* phase. The estimated (fit as a solid line in Fig. 2) value of critical exponent β_1 (in Eq. 1) is found to be 0.501 ± 0.001. The value of β_1 agrees with the mean field [45] prediction to underline the long range nature of the tilt order over the smectic layers.

The EC Effect in the SmC* Phase

A homogeneously aligned sample (in its SmC* phase) is obtained by applying 1 V of dc field and the extremely slow cooling (i.e., 0.01°C per min) of the sample from the isotropic phase to the $T_{N^*C^*}$.

Temperature variation of tilt angle (or its variation with field) is measured by optical extinction method in the SmC* phase. The variation of tilt angle with temperature and field are presented in Figs. 3 and 4, respectively. It is found that the tilt angle increases with field (at any temperature of interest) in SmC* phase. The field-induced tilt angle is found to attain a large value of 31° corresponding to an applied field of $1.1\,V\mu m^{-1}$. The observed variation of tilt angle with field (in the range of 0.04–1.1 V) in the SmC* phase is presented in Fig. 4. It is noticed that the EC effect is more pronounced in the vicinity of the N*C* phase transition. The influence of field (at $T_{N^*C^*}$) is argued due to the susceptibility of tilt fluctuations in the vicinity of the critical region. It may be noticed that the theoreticians [14–17] adopted the Generalized Landau Mean field theory to explain the strong dependence of induced tilt angle (EC-effect) in the SmC* phase at low fields. The EC-effect in the SmC* phase is

$$\begin{aligned} d\theta &\propto dE \\ d\theta &= \Theta \cdot dE \end{aligned} \tag{2}$$

where Θ is called the EC coefficient ($deg.V^{-1}\,cm$).

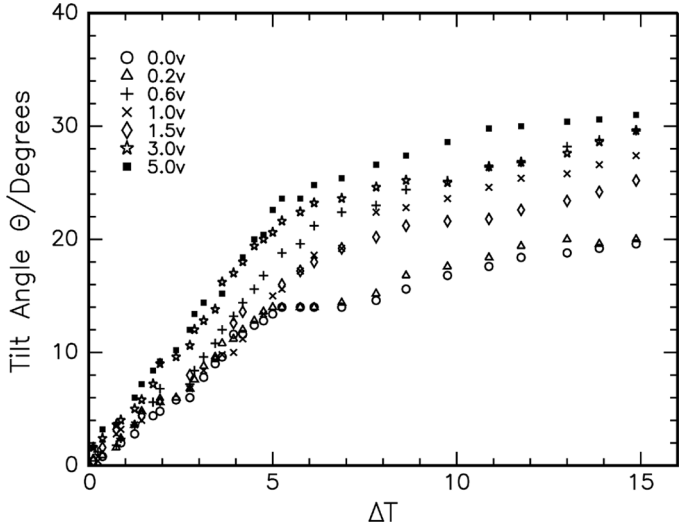

FIGURE 3 Temperature variation of tilt angle (at specified field) exhibited by 12 bpa.

The value of Θ estimated from observed EC-effect in the SmC* phase of 12 bpa at different temperatures is presented in Table 1. From the data, the variance is observed to be negligible (up to 2°C

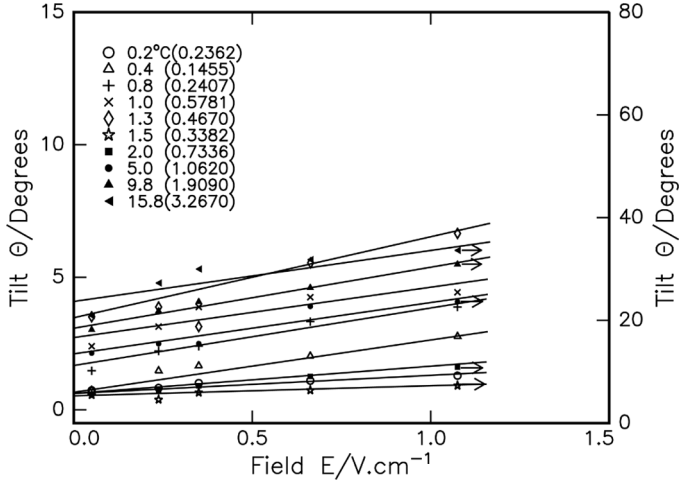

FIGURE 4 Field variation of tilt angle (at specified ΔT) in 12 bpa.

TABLE 1 Data of Electro-Clinic Effect (at Different Temperatures) in SmC* Phase

Temperature (ΔT)	Electro-clinic coefficient Θ value (deg.V^{-1} cm)
0.2	0.2362
0.4	0.1455
0.8	0.2407
1.0	0.5781
1.3	0.4670
1.5	0.3382
2.0	0.7336
5.0	1.0620
9.8	1.9090
15.8	3.2670

below $T_{N^*C^*}$). It may be noticed that EC-effect can be tuned effectively in the vicinity of the N^*C^* transition. It is also implied that, the coupling between the field and tilt becomes weaker as one moves away from the critical region (for $>2^\circ$C). The induced tilt angle θ(E) in the 12 bpa is found to be as large as 10°. This is found to be the largest EC-effect, so far reported [12–17] in other LCs in their SmC* phase or deVries SmA* phase. The present case of device friendly large EC-effect in 12 bpa is attributed to the presence of H-bonding. It is also explained basing on the following refined anisotropic dipole model (in Template-1). It is obvious that although HB is inclined to the-longitudinal axis, its projection on to the μ_l is considerable. It is also true that the soft-covalent interaction is relatively weaker. As the EC-effect now refers to the distortion of weakly coupled chemical moieties along μ_l, it is accompanied with a larger value.

Temperature Variation of Spontaneous Polarization in SmC* Phase

The detailed temperature variation of P_S(T) in SmC* phase of 12 bpa is presented in Fig. 5. The appearance of P_S current peak in SmC* phase confirms [28] its ferroelectric nature. The P_S is found to increase with decreasing temperature. Since, P_S is originated due to the finite tilt in SmC* phase, it is considered to be a secondary order parameter (i.e., tilt angle represents primary order parameter) in SmC* phase. The P_S in the SmC* is found to attain a maximum value of $\sim 6\,nC \cdot cm^{-2}$. This is relatively a lower value than that reported [27,38,42,43, 46–49] in other FLCs. Although, H-bonding in LCs is known [36,50] to enhance [29,43] transverse dipole moment to increase the stability [29,36] of the tilted phases, the P_S is found to be a relatively lower

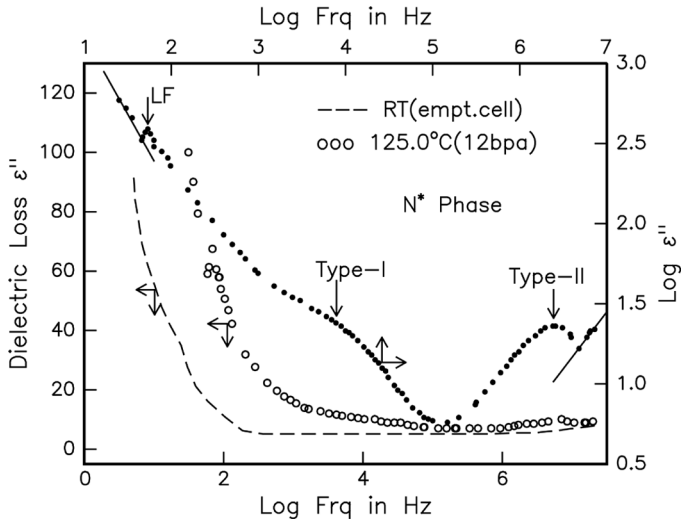

FIGURE 5 Frequency variation of dielectric loss ε'' exhibited by 12 bpa and empty cell in the N^* phase at 125.0°C.

value. The observed trend of lower value of P_S in the present HBFLC (viz., 12 bpa) is found to agree with that reported [28] trend of P_S value exhibited by standard inorganic ferroelectrics possessing H-bonding. The strikingly lower P_S in the present HBFLC than in other [27,36, 38,41] FLCs is argued due to the placement of chiral centre from the conjugated environment (of rigid core part) in the molecular frame leading to weaker coupling between them. As the coupling between the chiral centre and conjugation is weak, it leads to a lower P_S. The present 12 bpa is found to exhibit a lower P_S value compared to that reported [51] in the AFLCs with extended conjunction along the molecular frame. The lesser value of Ps in 12 bpa in comparison with 11 bpa [35] is due to the fact that present compound [29,39] is an even homologue.

The overall effect of the H-bonding in 12 bpa is found to:

i) Shift the thermal stability towards lower temperatures for device ambiance;
ii) Realize a lower value of spontaneous polarization;
iii) Induce a large tilt angle for wide viewing angle.

Further, even homologues are known [22,39] to project less μ_t. An overview of the data [51] in polymeric HBFLCs reveals that the involvement of the siloxane spacer leads to higher P_S values than that observed in the present case. However, the thermal stability of

ferroelectric SmC* phase exhibited [52] by other HBFLCs involving chiral stilbazoles (or mesogenic benzoic acids) is found to be comparable to that of the present 12 bpa.

The P_S in SmC* phase is found to increase with decreasing temperature. Increase of P_S is considered as growth of secondary order parameter. The growth is estimated by fitting the data to the relation given by

$$\begin{aligned} P_S(T) &\propto (\Delta T)^{\beta_2} \\ P_S(T) &= B \cdot (\Delta T)^{\beta_2} \end{aligned} \tag{3}$$

where $\Delta T = |T_{N^*C^*} - T_i|$, $T_{N^*C^*}$ is the chiral nematic to SmC* phase transition temperature, and T_i is the temperature of interest in SmC* phase.

The estimated value of β_2 is found to be 0.46 ± 0.001. The value of exponent is found to deviate from the Mean Field [45] prediction. The deviation is attributed to the inherently secondary nature of Ps in the case of SmC* phase.

Collective Excitations and Dielectric Relaxations in N* and C* Phases

Although $\varepsilon'(\omega)$ is found to monotonically decrease, the dielectric loss $\varepsilon''(\omega)$ (in both of the LC phases) seems to accompany with peak and valley values (or accompanied with a change in slope) respectively, with the increasing frequency. Representative variation of $\varepsilon''(\omega)$ in N* and C* phases is provided in Figs. 5 and 6, respectively.

Elimination of non-LC contributions is carried out as reported [35] earlier. The increasing loss $\varepsilon''(\omega)$ manifested as a peak value (or a change in its slope, i.e., through a point of inflexion) is considered to involve a relaxation process. The plots for $\varepsilon''(\omega)$ presented (for N* and C* phases) in Figs. 5 and 6, it is noticed that loss increases with frequency towards both the lower (<50 Hz) and higher (>6 MHz) limits. A meticulous observation of Figs. 5 and 6 further reveals that these increasing trends are additional contributions [46,53,54] rather than the relaxations exhibited by the LC. Although, the LC-relevant relaxations are labelled as LF, GM, Types I and II etc (with inset arrows in Figs. 5 and 6), the non-LC contributions (viz., due to possible conductive coating or ionic impurities) are resolved by the following procedure, viz.,

i) Drawing the log-log plot (as inset with right side Y-axis and top X-axis) of Figs. 5 and 6;
ii) Plotting the empty cell response for $\varepsilon''(\omega)$.

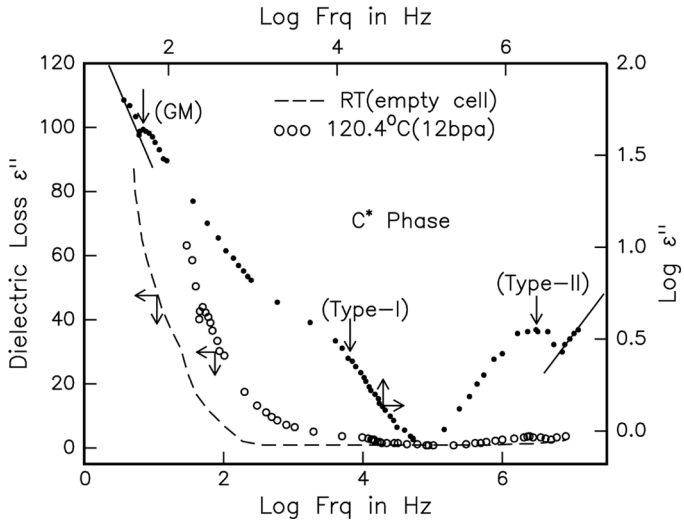

FIGURE 6 Frequency variation of dielectric loss ε'' exhibited by empty cell (at RT) and 12 bpa cell in the SmC* phase (at 122.5°C).

The presence of non-LC contributions in the observed dielectric spectrum in the lower (towards 10 Hz) and higher (towards 13 MHz) ends of the spectrum are confirmed by fitting the observed loss $\varepsilon''(\omega)$ to the frequency given by

$$\varepsilon'' \propto \{\mathrm{f}\}^{\mathrm{n}} \tag{4}$$

where f is the frequency.

The 'n' values estimated by the fitting (as inset solid lines in Figs. 5 and 6) procedure are found to be -0.75 and -0.95 (in N* phase); and 0.94 and 0.76 (in C* phase) for lower and higher frequency sides, respectively. In the wake of the LF dielectric reports [46,53,54] and the present case of slope values, it is confirmed that the increasing trends of ε'' (towards 10 Hz and towards 13 MHz) are due to the trace level ionic impurities and conductive coating (ITO) on the cell plates, respectively.

An overview of values in Figs. 5 and 6 along with the ε'' values of empty cell clearly indicates that the earmarked (by inset arrows in Figs. 5 and 6) low frequency mode, the GM, Types I and II relaxations are originated due to the LC contributions.

The assignments of Types I, II and GM are detailed in the following (Template-1) refined dipole model. Further, the loss spectrum $\varepsilon''(\omega)$ exhibited by 12 bpa at different temperatures is presented in Fig. 7

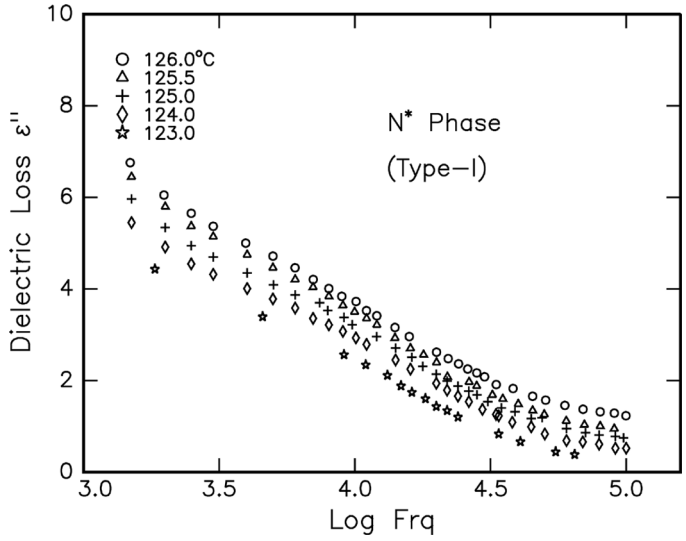

FIGURE 7 Frequency variation of dielectric loss ε'' exhibited by 12 bpa in the N^* phase for Type I relaxaion.

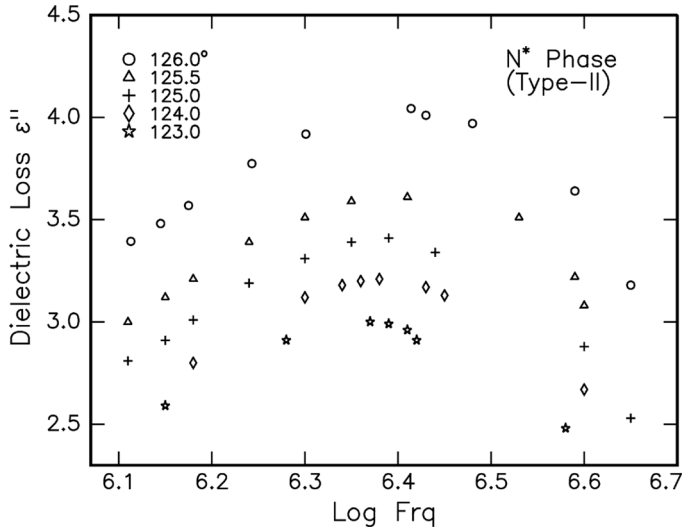

FIGURE 8 Frequency variation of dielectric loss ε'' exhibited by 12 bpa in the N^* phase for Type II relaxaion.

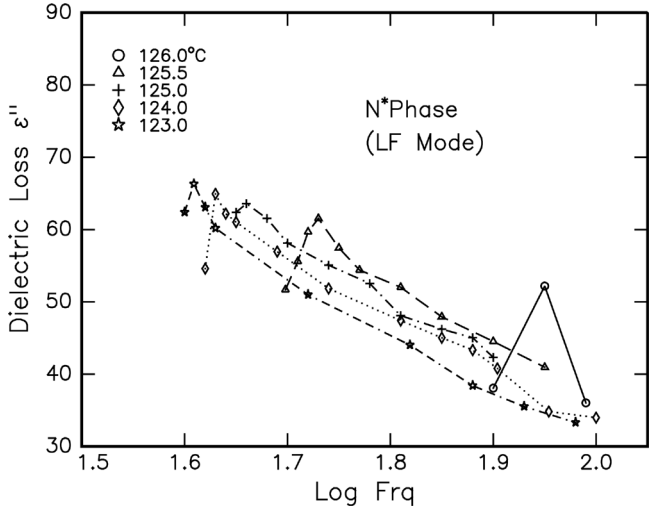

FIGURE 9 Frequency variation of dielectric loss ε'' exhibited by 12 bpa in the N^* phase for LF-relaxation.

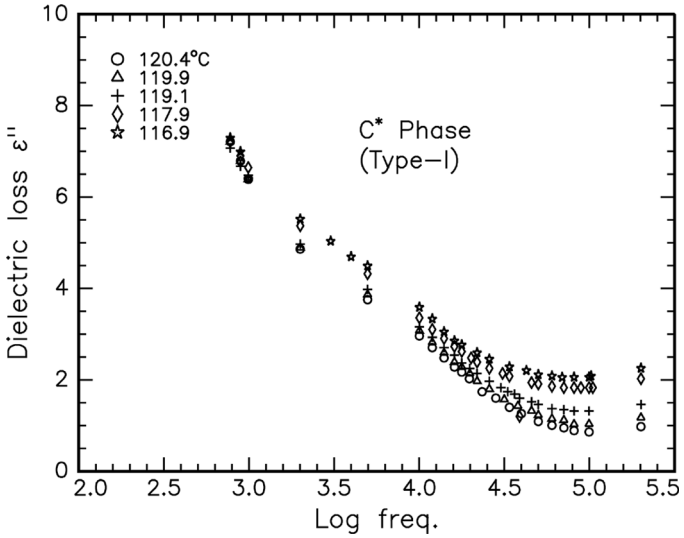

FIGURE 10 Frequency variation of dielectric loss ε'' exhibited by 12 bpa in the SmC^* phase for Type I relaxaion.

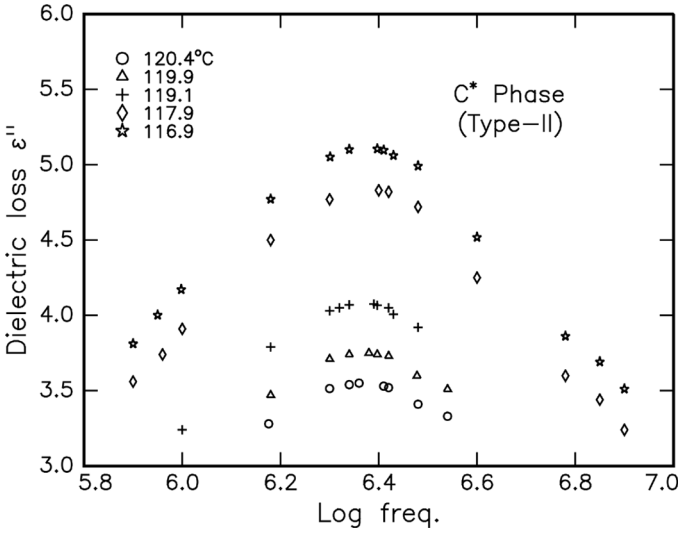

FIGURE 11 Frequency variation of dielectric loss ε'' exhibited by 12 bpa in the SmC* phase for Type-II relaxation.

(for Type I) and 8 (for Type II); Fig. 9 (for GM), −10 (for Type-I) and −11 (for Type-II) in N* and C* LC phases, respectively. The variation of loss for GM mode in Sc* phase is provided in Figure 12. The frequency at which ε'' attains maximum value is considered as the relaxation frequency f_R. The f_R is found to shift with temperature in N* and SmC* phases. The data of $f_R(T)$ observed for 12 bpa is presented in Table 2. It is also noticed that two types of relaxations occur in N* phase, while three types of relaxations occur C* phase.

The LF relaxation ($f_R < 100$ Hz) observed in C* phase is interpreted [47] as the collective response of the transverse dipole moment μ_t which is coupled over smectic layers. As such, this relaxation is identified [46] as GM mode. The order of f_R for the GM in 12 bpa is found to agree with that reported [35,42,43,46,47] in other FLCs. The values (Table 2) of f_R fall rather in the lower frequency side.

It is also noticed that values of f_R for GM in SmC* phase of 12 bpa are marginally lower than that reported [45] in 11 bpa. The values reported for f_R in N* phase are found to be higher than that for GM in the SmC* phase of the same compound. It is noticed that the GM for N* phase is reported for the first time in the case of 12 bpa. The relatively high f_R in N* phase (than in SmC*) of 12 bpa is argued as due to the lower viscosity in higher temperature N* phase. The observations of LF mode in N* phase is suggestive of a possible coupling of μ_t.

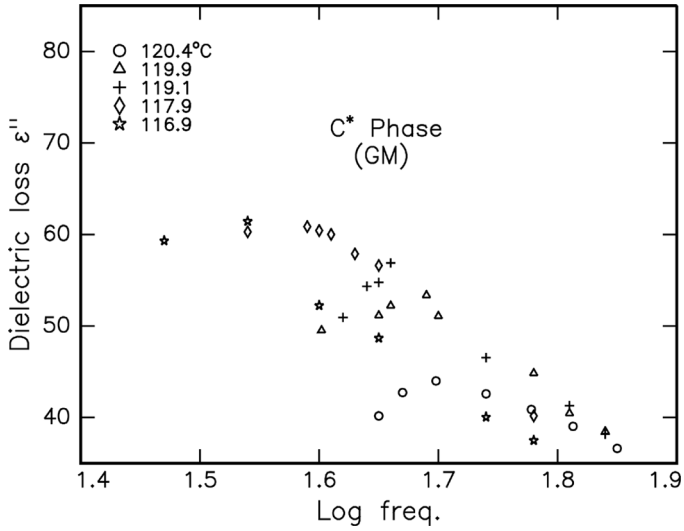

FIGURE 12 Frequency variation of dielectric loss ε'' in the SmC* phase for GM-mode.

The influence of applied field on GM relaxation in C* phase is studied. The f_R and $\varepsilon''(\omega)_{max}$ are found to vary with the field. The observed shift of f_R with field is presented in Fig. 13. The variation (suppression) of loss $\varepsilon''(\omega)_{max}$ with field confirms the fact that GM is originated from the coupling of μ_t with field over smectic layers. The

TABLE 2 Data of Relaxation Frequency f_R and Dielectric Loss Maximum ε''_{max} in N* and C* Phases

		LF/GM		Type-I		Type-II	
LC Phase	T°C	f_R Hz	ε''_{max}	f_R KHz	ε''_{max}	f_R MHz	ε''_{max}
N*	126.0	90.03	52.19	4.99	4.73	2.60	4.04
	125.5	53.94	61.54	4.00	4.73	2.57	3.61
	125.0	45.98	63.58	3.00	4.70	2.50	3.41
	124.0	43.04	64.94	2.50	4.55	2.40	3.21
	123.0	40.62	66.30	1.83	4.42	2.36	3.00
SmC*	120.4	{50.02}	43.96	13.98	2.48	2.31	3.55
	119.9	{48.98}	53.53	11.95	2.82	2.39	3.75
	119.1	{45.98}	56.84	10.03	3.16	2.45	4.08
	117.9	{38.98}	60.92	4.97	4.29	2.49	4.82
	116.9	{34.98}	61.53	1.99	5.51	2.51	5.10

{ } refers to GM mode in SmC*phase.

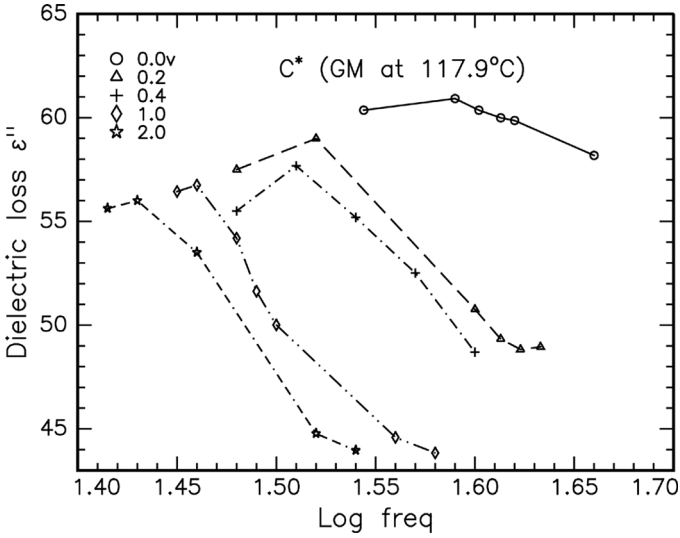

FIGURE 13 Frequency variation of dielectric loss ε'' at different fields in SmC* phase (at 120.0°C) relevant to GM-mode for 12 bpa.

variation of dielectric loss ε''_{max} and the shift of f_R are presented in Table 3. The f_R is found to shift towards lower frequency side with the increasing field. This trend of f_R is found to agree with the experimental reports [35,42,43,46,47] in the C* phase exhibited by other FLCs.

The other two relaxations corresponding to the peaks in ε'' (one ~10 KHz and other ~1 MHz) are labelled as Type-I and Type-II relaxations, respectively. They are presented in Figs. 5 and 6 in N* and C* phases. They are related to the reorientation mechanism of longitudinal dipole moment μ_l to the applied field as explained by the following refined dipole model (Template 1). The present case of 'Multiple Relaxations' is found to be analogous to that reported [53,54] in the nematic and smectic phases of other calamitic LCs. In

TABLE 3 Data for Field Variation of GM Relaxation Frequency f_R and loss Maximum ε''_{max} in SmC* Phase

Bias in volts	f_R Hz	ε''_{max}
0.0	39.00	60.92
0.2	33.41	58.99
0.4	32.18	57.68
1.0	29.01	56.75
2.0	26.99	55.99

a similar way, the present multiple relaxations (Type-I and -II) are attributed to the distinct response of μ as shown in the Template 1.

Refined Dipole Model and Re-Orientation Mechanism

The response of molecular dipole moment is addressed through the following refined dipole model for the 12 bpa molecule in the following way. The dipole moment μ associated with H-bonded LC molecule is resolved into the different components as illustrated in the Template 1.

As per the refined dipole model, the dipole moment μ can be resolved into:

i) the longitudinal dipole moment μ_1 situated along rigid core part of molecule
ii) the longitudinal dipole moment μ_l situated at the flexible part of molecule along electro negative Oxygen atom and
iii) the transverse dipole moment μ_t situated (away from μ_1) at the chiral center inclined to molecular long axis.

The Type-I (lower frequency) relaxation is attached to the reorientation of μ_1 associated with the flexible end chain. Flexibility leads to the slow reorientation. Thus, it is noticed that Type-I relaxation time (Table 2) is observed to be lower (than type-II) to agree with the expectations of the present dipolar model. As the Type-II relaxation (higher frequency, fast) is attached to the reorientation of μ_1 pertaining to the rigid core part, it is expected to be fast. It is also noticed that Type-II relevant f_R (Table 2) bears higher values to agree with the present refined dipolar model.

The variation of $f_R(T)$ for all the relaxations (i.e., GM, Type-I, Type-II) in the N^* and C^* phases is presented in Figure 14. The variation is found to be analogous to the reported [42,43,46,47] cases of f_R across AC^* transition.

The decreasing trend of f_R (viz., regarding the LF, Type-I and Type-II in N^* and GM and Type-I C^* phases) with decreasing temperature is suggestive of an Arrhenius [25,26] type of behaviour. But, the $f_R(T)$ of GM in SmC^* phase is not considered as Arrhenius shift, since this mode represents a collective response. The interesting, but intriguing trend of increasing f_R with the decreasing temperature for Type-II relaxation is found in C^* phase. An overall trend of decreasing $f_R(T)$ for Type-II implies the softening of amplitude towards the transition temperature $T_{N^*C^*}$. Hence, this Type-II relaxation in C^* phase is considered as Soft Mode. It is found that the magnitude of f_R regarding

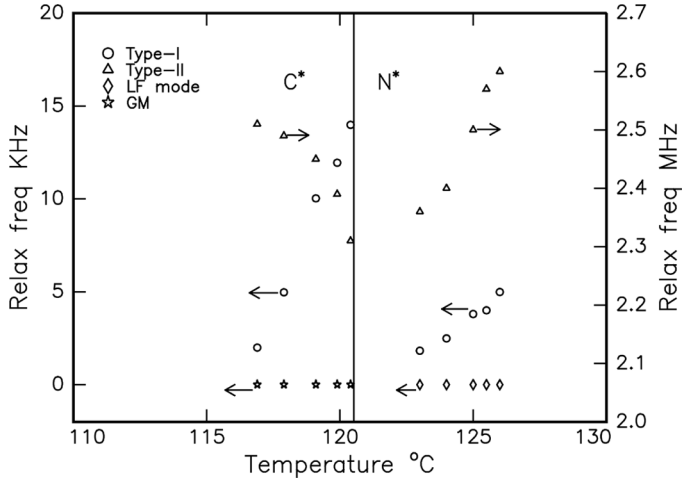

FIGURE 14 Temperature variation of relaxation frequency f_R for LFmode, GM, Type-I, and Type-II relaxations in 12 bpa.

the SM (Type-II) relaxation (for $T<T_{N^*C^*}$) agrees with the reported [42,43,46,47] values in other FLCs in the vicinity of $T_{AC}{}^*$. Since, SM is also considered as collective motion, the corresponding variation of f_R is not considered for Arrhenius shift.

The temperature variation of dielectric increment $\Delta\varepsilon(T)$ pertaining to Type-II relaxation in C^* phase (in the vicinity of N^*C^* phase transition, i.e., for $T<T_{N^*C^*}$) is found (Figure 15) to exhibit Curie-Weiss behaviour [28] given by

$$\begin{aligned} \Delta T &\propto [1/(\Delta\varepsilon)^{\gamma-1}] \\ \Delta T &= G \cdot [1/(\Delta\varepsilon)^{\gamma-1}] \end{aligned} \tag{5}$$

The estimated value of γ is (by fitting the data of Type-II relaxation in C^* phase to Eq. 7) is found to be 1.015 ± 0.001 for $T < T_{N^*C^*}$, i.e., during the growth [28,46] of ferroelectric domains (in the vicinity of $T_{N^*C^*}$) with decreasing temperature.

The Type-I relaxation in N^* and C^* phases and Type-II relaxation in N^* phase are found to exhibit Arrhenius behaviour. The corresponding activation energies are estimated through the reduced temperature plots (Fig. 16). The activation energies are found to be 6.39 eV (Type-I) and 0.69 eV (Type-II) in N^* phase; 10.65 eV (Type-I) in SmC^* phase. It is noticed that the activation energy for Type-I relaxation is higher than that of Type-II relaxation in N^* phase. The μ_1 relevant to the Type-I relaxation is attached to the molecular long axis. Since, the

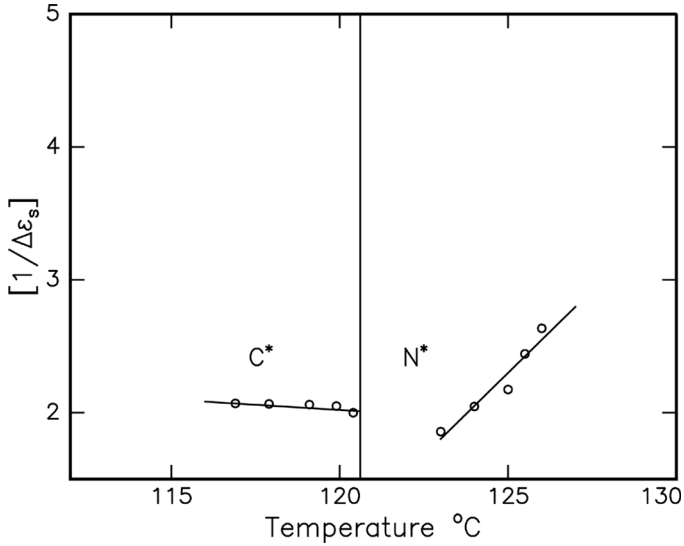

FIGURE 15 Temperature variation of dielectric increment $\Delta\varepsilon$ relevant to Soft-mode in SmC* phase along with Type-II in N* phase for 12 bpa.

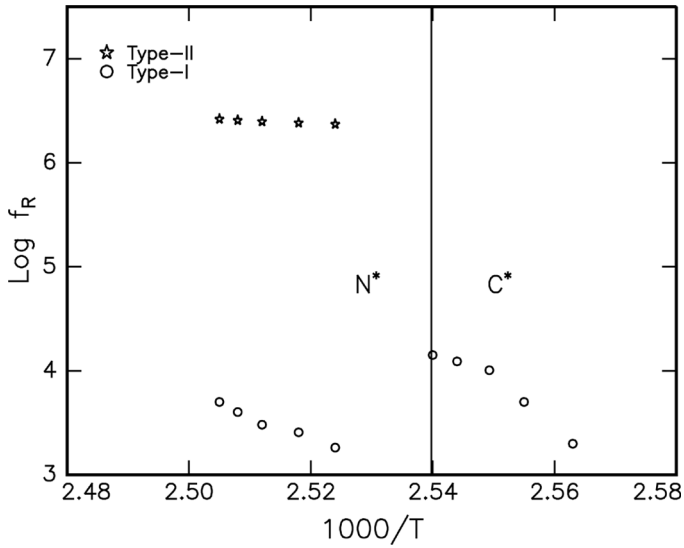

FIGURE 16 Arrhenius plots in N* and SmC* phases exhibited by 12 bpa.

Type-I relaxation is relevant to the reorientation of dipole attached to the flexible part of molecule, a higher potential (orientational) barrier is expected for its alignment to the field. However, Type-II relevant activation energy is found to bear lower value in N* phase. The activation energy relevant to Type-II refers to the reorientation mechanism of μ_1 situated in the rigid core part of the molecule. As per the refined dipole model (Template 1), the component of μ_1 for Type-II appears to be favourably aligned to the molecular long axis. Therefore, it experiences a small potential barrier to reorient to the applied field. The overall higher value of activation energy in SmC* phase than that in the N* phase reflects upon the relatively fixed confinement of the longitudinal dipole μ_1 in SmC* phase. Although the order of activation energy in 12 bpa is comparable to that reported [35,42,43,47] in other FLCs, an overview of the data (in N* and SmC*) is indicative of higher activation energy (potential barrier) in the present HBFLCs. It is also noticed that activation energies in 12 bpa are found to be higher than that reported [35] for 11 bpa. The higher activation energy is argued due to the relatively inclined soft-covalent interaction in the H-bond with respect to the molecular long axis. It is concluded that of H-bond in LCs leads to higher orientation potential barrier to indicate higher threshold voltages required to operate an HBFLC device.

The dielectric dispersion, viz., $\varepsilon''(\omega)$ versus $\varepsilon'(\omega)$ studied at different temperatures (for Type-I, Type-II, and GM) and fields for GM (as presented in Figs. 7–12) appears to be asymmetric about loss maximum, $\varepsilon''_{\max}$. Such asymmetric (or non-Debye's) type of off-centred dispersion is analyzed through the Cole–Davidson relation [25,26,55] given by

$$\varepsilon^*(\omega) = \varepsilon_\infty - [\Delta\varepsilon]/[1 + (j\omega\tau)^{1-\alpha}] \tag{6}$$

where $\Delta\varepsilon = [\varepsilon_0 - \varepsilon_\infty]$, the dielectric increment (or strength), $\omega = 2\pi f$ (where f is the frequency), $\tau =$ the relaxation time i.e., $1/f_R$, $\alpha =$ distribution parameter (or degrees of freedom) reflecting the constraints on the dipole and its fixation (in molecular frame) during the reorientation to the field.

The observed dispersal of $\varepsilon''(\omega)$ and $\varepsilon'(\omega)$ at different temperatures (relevant to the relaxations of interest) is represented as Cole-Cole plots. The corresponding Cole-Cole plots are presented in Figures 17 (for Type-I), -18 (for Type-II) and -19 for GM in N* phase; and Figures 20 (for Type-I), -21 (for Type-II) and -22 (for GM) for SmC* phase exhibited by 12 bpa. The Cole-Cole plots (i.e, field variation) for GM dispersion in SmC* of 12 bpa are presented in Figure 23.

The values of ε_o, ε_∞, α and the dielectric increment $\Delta\varepsilon$ are estimated from the Cole-Cole plots. The temperature variation of dielectric

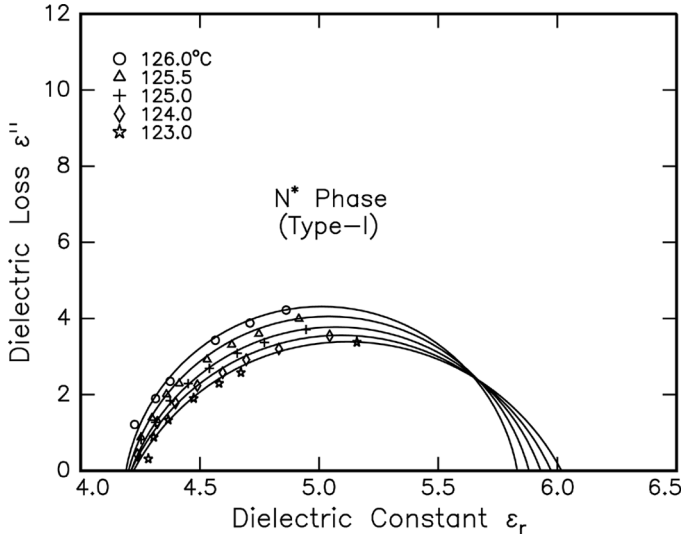

FIGURE 17 Cole-Cole plots for Type-I relaxation in N* phase for 12 bpa.

increment $\Delta\varepsilon$ and distribution parameter 'α' in N* and C* phases for 12 bpa are presented in Table 4. The $\Delta\varepsilon$ values in 12 bpa for GM in C* are found to be higher [35] than that Sc* phase of 11 bpa. The

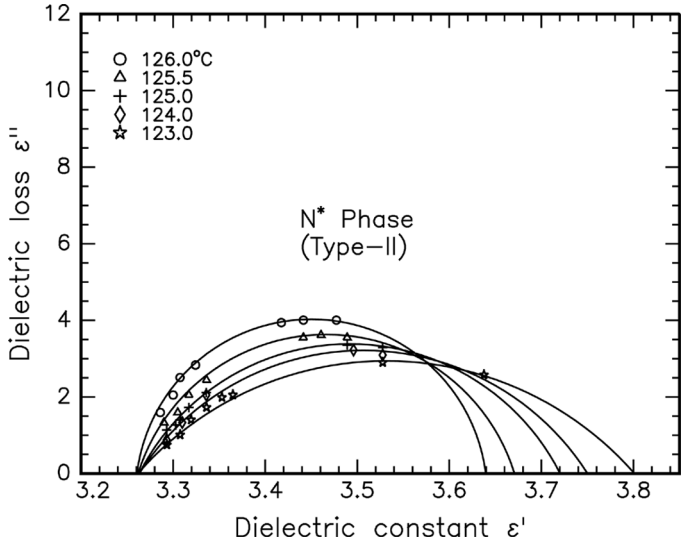

FIGURE 18 Cole-Cole plots for Type-II relaxation in N* phase for 12 bpa.

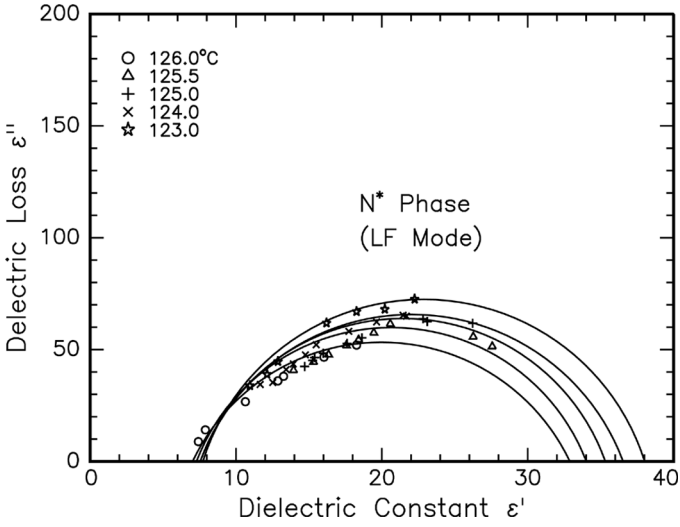

FIGURE 19 Cole-Cole plots for LF-mode relaxations at different temperatures in N^* phase for 12 bpa.

values of $\Delta\varepsilon$ for LF in N^* phase of the 12 bpa are found to be higher than that in Sc^* phase. An overview of α values reveals [35] higher values for 12 bpa than in 11 bpa. This higher α value in 12 bpa suggests

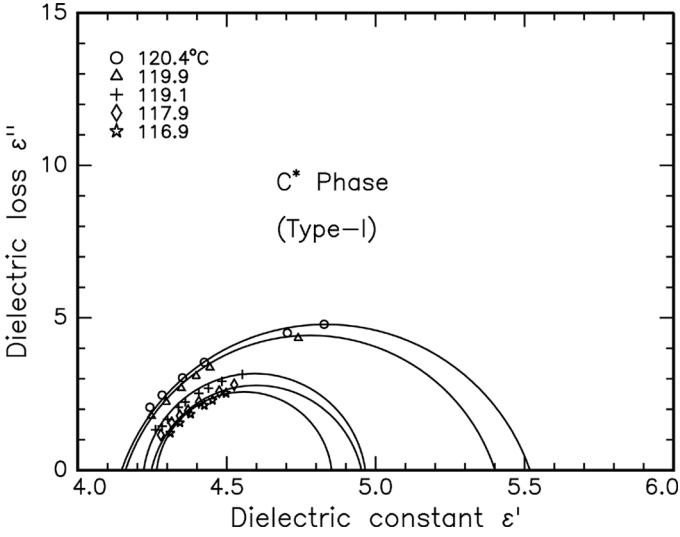

FIGURE 20 Cole-Cole plots for Type-I relaxation in SmC^* phase of 12 bpa.

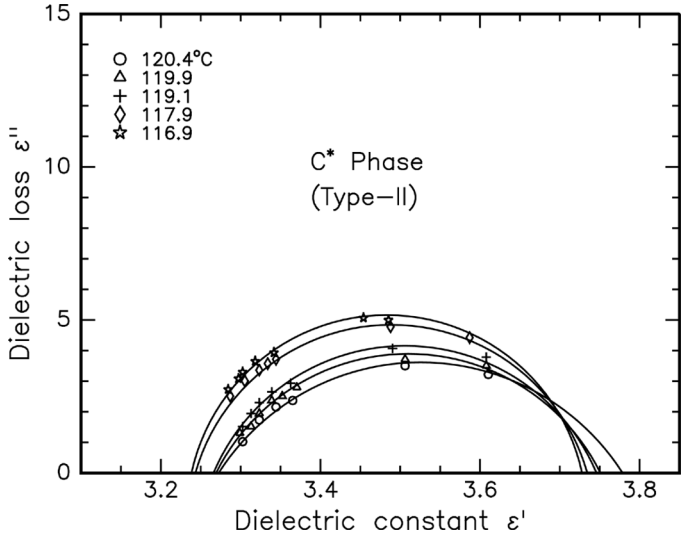

FIGURE 21 Cole-Cole plots for Type-II relaxation in SmC* phase for 12 bpa.

a strong confinement in the case of even homologue as a result of odd-even effect. The influence of applied field on dielectric increment $\Delta\varepsilon$ and α parameter regarding GM mode in SmC* phase for 12 bpa is presented in Table 5.

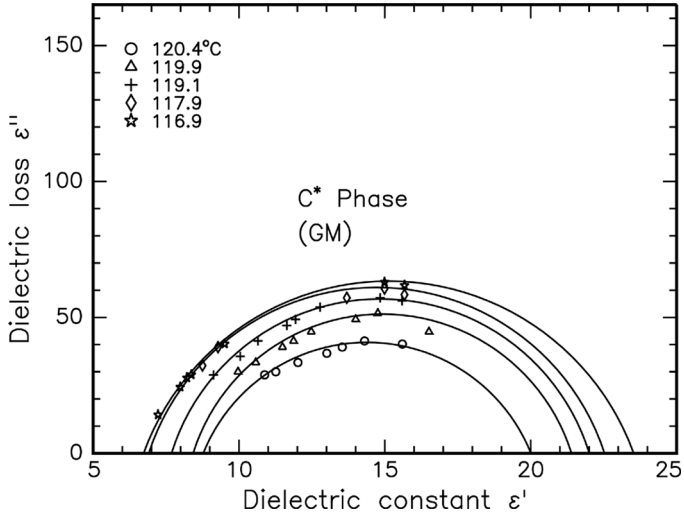

FIGURE 22 Cole-Cole plots for GM-mode relaxations at different temperatures in SmC* phase for 12 bpa.

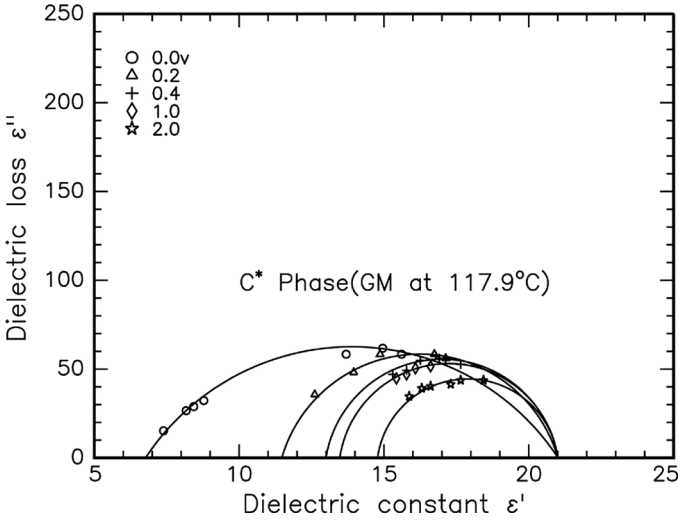

FIGURE 23 Cole-Cole plots for GM-mode at different voltages for 12 bpa in C* phase.

The estimated values of α relevant to Type-I, Type-II (involving individual dipole reorientation only) in N* phase reveal an overall increasing trend with decreasing temperature. The increasing α value with decreasing temperature reflects upon the increasing constraints experienced by the dipole. This trend of α-values reflect the fixation of dipole moment in the molecular body. But, the α-values in LF mode

TABLE 4 Data of Temperature Variation of Dielectric Increment $\Delta\varepsilon$ and α-Parameters in 12 bpa

		LF/GM		Type - I		Type - II	
LC Phase	T°C	$\Delta\varepsilon$	α_{rad}	$\Delta\varepsilon$	α_{rad}	$\Delta\varepsilon$	α_{rad}
N*	126.0	26.00	0.349	1.64	0.156	0.3795	0.0523
	125.5	26.80	0.314	1.68	0.244	0.4092	0.2616
	125.0	30.80	0.297	1.72	0.314	0.4598	0.3663
	124.0	31.00	0.279	1.75	0.348	0.4885	0.4361
	123.0	32.30	0.262	1.80	0.401	0.5380	0.4884
SmC*	120.4	{11.25}	0.3314	1.37	0.2965	0.500	0.4361
	119.9	{12.95}	0.2616	1.24	0.2791	0.486	0.3837
	119.1	{14.25}	0.2442	0.74	0.1918	0.485	0.3314
	117.9	{15.60}	0.2267	0.70	0.1744	0.484	0.3140
	116.9	{16.70}	0.2093	0.59	0.1570	0.483	0.2965

{ } refers to GM mode in SmC* phase.

TABLE 5 Data of Field Variation Data of Dielectric Increment $\Delta\varepsilon$ and α-Parameter in SmC* Phase

Bias in volts	$\Delta\varepsilon = [\varepsilon_0 - \varepsilon_\infty]$	α
0.0	14.30	0.896
0.2	9.50	0.529
0.4	8.00	0.366
1.0	7.50	0.354
2.0	6.25	0.326

in N* and GM in C* phases and that of Type-II in C* phase are not found to follow this trend. This anomalous trend is attributed to the interaction of μt with field as the LC phase stabilises.

It is found that the shift of dielectric increment $\Delta\varepsilon$ with temperature is pronounced at the low frequency (static) side of permittivity ε_0 in Cole-Cole plots. This trend is found to be more effective for the case of GM mode relaxation than that for Type-I and Type-II. The observed large temperature shift of $\Delta\varepsilon$ is argued as due to the underlying collective interaction of μ_t over smectic layers. It is also noticed (Fig. 23) that the shift in permittivity ε' with field is pronounced at the high frequency end at ε_∞ for GM.

However, the loss ε_{max} values (Fig. 13) are found to decrease with increasing field. The decrease in loss reflects the unwinding of polarization helix in SmC* phase. The GM relaxation frequency f_R (Table 2) is found to shift to higher frequency side with increasing temperature. But the variation of f_R with field (Table 3) is found to follow an opposite trend to imply that work is done by the field to unwind it. Thus, it is implied that the switching action can be triggered by applying optimum field. Applying field leads to unwinding the polarization helix, and the μ_t is released in SmC* phase for its switching. The observed trend of temperature variation of $f_R(T)$ is found to agree with the reports [35,42,43] in other FLCs. The decreasing trend of α-values (Table 5) with increasing field for GM in SmC* phase also reflects the release of transverse dipole from it being entangled in polarization helix.

CONCLUSIONS

The experimental investigations regarding P_S, Tilt Angle, and LF relaxations in 12 bpa reveal that H-bonding in the FLCs leads to:

1) Larger induced tilt angle, to suggest a wider viewing angle and better contrast ratio of the device;

2) Increased thermal stability (shifted towards ambient temperatures), but relatively low P_S value;
3) Pronounced EC-effect in the critical region of 2°C in the vicinity of the N^*C^* transition temperature to promote better contrast ratio;
4) Lower threshold value to utilise the P_S switching in device;
5) A higher potential barrier to speak out higher threshold energy (relevant to the longitudinal dipole moment) for device operation;
6) LF relaxation similar to GM in SmC^* phase is observed in chiral Nematic phase for the first time.

REFERENCES

[1] Clark, N. A., & Lagerwall, S. T. (1980). *Appl. Phys. Lett.*, *36*, 299; ibid: (1984). *Ferroelectrics*, 59, 25.
[2] Goodby, J. W., Blinc, R., Clark, N. A., Lagerwall, S. T., Osipov, M. A., Pikin, S. A., Sakurai, T., Yoshino, K., & Zeks, B. (1991). *Ferroelectric Liquid Crystals – Principles, Properties and Applications*, Gordon and Breach, Philadelphia.
[3] Nishiyama, I. (1994). *Adv. Mater*, *6*, 996.
[4] Ouchi, Y., Yoshioka, Y., Ishii, H., Seki, K., Kitamura, M., Noyori, R., Takanishi, Y., & Nishiyama, I. (1995). *J. Mater. Chem.*, *5*, 2292.
[5] Fukuda, A., Takanishi, Y., Isozaki, T., Ishikawa, K., & Takezoe, H. (1994). *J. Mater. Chem.*, *4*, 997.
[6] Johno, M., Itoh, K., Lee, J., Ouchi, Y., Takezoe, H., Fukuda, A., & Kusunoki, T. (1990). *Jpn. J. Appl. Phys.*, *29*, L107.
[7] Cluzeau, P., Ismaili, M., Anakkar, A., Foulon, M., Babeau, A., & Nguyen, H. T. (2001). *Mol. Cryst. Liq. Cryst.*, *362*, 185.
[8] D'have, K., Rudquist, P., Lagerwall, S., Pauwels, H., Drzewinski, W., & Dabrowski, R. (2000). *Appl. Phys. Lett.*, *76*, 3528.
[9] D'have, K., Rudquist, P., Matuszczyk, M., Lagerwall, S., Pauwels, H., & Dabrowski, R. (2000). In: *Liquid Crystal Materials, Devices and Flat Panel Displays*, Shashidhar, R. & Ganaade, B. (Eds.), Proc. SPIE, 3955, 33.
[10] D'have, K., Dahlgren, A., Rudquist, P., Lagerwall, J. P. F., Andrewsson, G., Mutuszczyk, M., Lagerwall, S. T., Dabrowski, R., & Drzewinski, W. (2000). *Ferroelectrics*, *244*, 115.
[11] Garoff, S., & Meyer, R. B. (1977). *Phys. Rev. Lett.*, *38*, 848.
[12] Meyer, R. B. (1977). Ferroelectric Liquid Crystals: A Review. *Mol. Cryst. Liq. Cryst.*, *40*, 33.
[13] Garoff, S., & Meyer, R. B. (1979). *Phys. Rev. A.*, *19*, 338.
[14] Zeks, B., & Stefan, J. (1984). *Mol. Cryst. Liq. Cryst.*, *114*, 259.
[15] Carlsson, T., Zeks, B., Filipic, C., Levstik, A., & Blinc, R. (1988). *Mol. Cryst. Liq. Cryst.*, *163*, 11.
[16] Zeks, B., & Blinc, R. (1991). In: *Ferroelectric Liquid Crystals*, Gordon & Breach, (Ed.), Philadelphia, 365.
[17] Abdulhalim, I., & Moddel, G. (1991). *Liq. Cryst.*, *9*, 493.
[18] Collings, N., Crossland, W. A., Chittick, R. C., & Bone, M. F. (1989). *Proc. SPIE*, *963*, 46.
[19] Andersson, G., Dahl, I., Komitov, L. Lagerwall, S. T., Skarp, K., & Stebler, B. (1989). *J. Appl. Phys.*, *66*, 4983.

[20] Williams, P. A., Clark, N. A., Ros, M. B., Walba, D. M., & Wand, M. D. (1991). *Ferroelectrics*, *121*, 143.
[21] Ratna, B. R., Crawford, G. P., Prasad, S. K., Naciri, J., Keller, P., & Shashidhar, R. (1993). *Ferroelectrics*, *148*, 425.
[22] Wang, J. M., Kim, Y. J., Kim, C. J., & Kim, K. S. (2002). *Ferroelectrics*, *277*, 185.
[23] Aira, H., Ray, H., & Kohki, T. (2004). *Jpn. Jr. Appd. Phy. Part-I*, *43*(9A), 6243.
[24] Wu, S. L., & Lin, C.-Y. (2003). *Liq. Cryst.*, *30*, 205.
[25] Hills, N. E., Wanghan, W. E., Price, A. H., & Davies, M. (1969). In: *Dielectric Properties and Molecular Behaviour*, Van Nostrand (Ed.), New York.
[26] Jonscher, A. H. (1983). In: *Dielectric Relaxations in Solids*, Chelsea Dielectrics Press: London.
[27] Kumar, P. A., & Pisipati, V. G. K. M. (2000). *Advc. Mater.*, *2*, 1617.
[28] Kittel, C. (2005). In: *Introduction to Solid State Physics*, 7th ed., John Wiley & Sons, Inc.: New York.
[29] Luckhurst, G. R., & Gray, G. W. (1979). In: *The Molecular Physics of Liquid Crystals*, Academic Press: New York, Chap. 12.
[30] Niori, T., Sekine, T., Watanabe, J., Furukawa, J., Choi, S. W., & Takezoe, H. (1996). *J. Matter. Chem.*, *6*, 1231.
[31] Niori, T., Sekine, T., Watanabe, J., Furukawa, J., Choi, S. W., & Takezoe, H. (1997). *J. Mater. Chem.*, *7*, 1307.
[32] Kato, T., & Frechet, J. N. J. (1989). *J. Am. Chem. Soc.*, *111*, 8533.
[33] Kihara, H., Kato, T., Uryu, T., Ujiie, S., Kumar, U., Frechet, J. M. J., Bruce, W. D., & Price, J. D. (1996). *Liq. Cryst.*, *21*, 25.
[34] Brand, H. R., Cladis, P. E., & Pleiner, H. (1992). *Macro Mol.*, *25*, 7223.
[35] Sreedevi, B., Chalapathi, P. V., Kotikalapudi, V. K. M., Pisipati, V. G. K. M., & Potukuchi, D. M. (2007). *Ferroelectrics*, *361*, 18.
[36] Sreedevi, B., Chalapathi, P. V., Srinivasulu, M., Pisipati, V. G. K. M., & Potukuchi, D. M. (2004). *Liq. Cryst.*, *31*, 303.
[37] Madhumohan, M. L. N., Goud, B. V. S., Kumar, P. A., & Pisipati, V. G. K. M. (1999). *Mater. Res. Bullt.*, *34*, 2167.
[38] Noot, C., Perkins, S. P., & Coles, H. J. (2000). *Ferroelectrics*, *244*, 331.
[39] Marcelja, P. (1974). *J. Chem. Phys.*, *60*, 3599.
[40] Stipetic, A. I., Goodby, J. W., Hird, M., Raoul, Y. M., & Gleeson, H. F. (2006). *Liq. Cryst.*, *33*, 819.
[41] McDonald, R., Lacey, D., Watson, P., Cowling, S., & Wilson, P. (2005). *Liq. Cryst.*, *32*, 319.
[42] Potukuchi, D. M., Goud, B. V. S., & Pisipati, V. G. K. M. (2002). *Ferroelectrics*, *265*, 279; ibid: (2003) *289*, 77.
[43] Potukuchi, D. M., George, A. K., Carboni, C., Al-Harthi, S. H., & Naciri, J. (2004). *Ferroelectrics*, *300*, 1.
[44] de Gennes, P. G. (1974). In: *The Physics of Liquid Crystals*, Marshall Wilkinson, (Ed.), Clarendon Press: Oxford.
[45] Stanley, H. E. (1971). In: *Introduction to Phase Transition and Critical Phenomena*, Clarendon Press.
[46] Gouda, F., Skarp, K., & Lagerwall, S. T. (1991). *Ferroelectrics*, *113*, 161.
[47] Potukuchi, D. M., George, A. K., Carboni, C., Al-Harthi, S. H., & Naciri, J. (2004). *Mol. Cryst. Liq. Cryst.*, *409*, 343.
[48] Andersson, G., Dahl, I., Keller, P., Kuczinski, W., Lagerwall, S. T., Skarp, K., & Stebler, B. (1987). *Appl. Phys. Lett.*, *51*, 640.
[49] Madhumohan, M. L. N., & Pisipati, V. G. K. M. (1999). *Liq. Cryst.*, *26*, 1609.
[50] Paleos, C. M., & Tisiourvas, D. (2001). *Liq. Cryst.*, *28*, 1127.

[51] Kumar, U., Frechet, J. M. J., Kato, T., Ujiie, S., & Timura, K. (1992). *Angew. Chem. Int. Ed. Engl.*, *31*, 1531.
[52] Kato, T., Kihara, H., Uryu, T., Ujiie, S., Timura, K., Frechet, J. M. J., & Kumar, U. (1993). *Ferroelectrics*, *148*, 161.
[53] Kress, H., Tschierske, S., Hohmuth, A., Stotzer, C., & Weissflog, W. (1996). *Liq. Cryst.*, *20*, 715.
[54] Rani, G. P., Potukuchi, D. M., & Pisipati, V. G. K. M. (1998). *Liq. Cryst.*, *25*, 589.
[55] Cole, R. H. (1941). *J. Chem. Phys.*, *9*, 341.